Direct *ab initio* molecular dynamics study on the reactions of multi-valence ionized states of water dimer

Tomoya Takada[1] and Hiroto Tachikawa[2]

[1] Department of Applied Chemistry and Bioscience, Chitose Institute of Science and Technology, Chitose 066-8655, Japan
[2] Division of Applied Chemistry, Faculty of Engineering, Hokkaido University, Sapporo 060-8628, Japan

E-mail: t-takada@photon.chitose.ac.jp

Received xxxxxx
Accepted for publication xxxxxx
Published xxxxxx

Abstract

We investigated the reaction of multi-valence (+2) ionization states of water dimer $(H_2O)_2$ using direct *ab initio* molecular dynamics (AIMD) method. The following multi-valence ionization states were considered. In the direct two-electron ionization state, $(H_2O)_2$ was ionized to form $(H_2O)_2^{2+}$ in one step; in the stepwise two-electron ionization state, $(H_2O)_2$ was first converted to $(H_2O)_2^{+}$ and further ionized after structural relaxation. The $(H_2O)_2^{2+}$ from direct ionization dissociated into two H_2O^+ ions, while $(H_2O)_2^{2+}$ in stepwise ionization generated H_3O^+ and OH^+ ions from H_3O^+–OH radical-ion pairs. Additionally, we performed dynamics calculations for the excited state of $(H_2O)_2^{2+}$ generated through direct ionization. The excited $(H_2O)_2^{2+}$ ions also dissociated to form H_3O^+ and OH^+ ions. The reaction mechanism of multi-valence ionization states of $(H_2O)_2$ is discussed on the basis of calculation results.

Keywords: direct *ab initio* molecular dynamics, water dimer, multi-valence ionization, dissociation product

Supplementary materials for this article are available online

(Some figures may appear in colour only in the online journal)

1. Introduction

The ionization of water clusters is an important phenomenon in astrophysics and astrochemistry. For example, solid water in a comet is predicted to be amorphous ice [1-5], similar to aggregated water clusters. When the comet approaches the sun, the clusters are ionized upon irradiation with cosmic rays from the sun [6-13]. Information on the ionization dynamics is therefore essential for understanding the chemical processes occurring in the ice of the comet. Moreover, the ionization of water clusters is important in the fields of radiation-induced processes in nuclear atomic plants and photochemical reactions progressing in the atmosphere [14-16]. For example, many initial events of radiation-induced chemical reactions related to water-containing systems involve the ionization of water.

The ionization effects of water have been extensively studied using various spectroscopic techniques. Shinohara et al. detected the generation of molecular clusters in an irradiated water-argon mixture supersonic jet by means of mass spectroscopy [17, 18]. They found protonated cation

$H^+(H_2O)_n$ and unprotonated cation $(H_2O)_n^+$ after the ionization. Mizuse et al. studied the structure of gaseous water cluster cations using infrared spectroscopy [19-22]. They found that the spectroscopic characteristics of the free OH stretching modes are similar to those of $H^+(H_2O)_n$, suggesting that $(H_2O)_n^+$ exists in the form of $H^+(H_2O)_{n-1}(OH)$ with a network structure similar to that of the protonated cation.

The ionization of water clusters has also been studied theoretically. Barnett and Landman found stable structures of $(H_2O)_n^+$ by means of *ab initio* calculations [23]. Their calculations revealed that a proton-transferred complex (H_3O^+–OH) exists in all the examined clusters. Similar results were reported by Lee and Kim [24]. Svoboda et al. reported on the basis of non-adiabatic dynamics simulations that the H_3O^+–OH and dissociated products (H_3O^+ + OH•, H_3O^+• + H_2O, H• + OH• + H_2O^+•; dots denote unpaired electrons of radical and radical cations) are formed from $(H_2O)_2^+$, and their yields depend on the populated electronic state of $(H_2O)_2^+$ [25]. Herr et al. studied the ionization of water clusters consisting of 1–21 molecules and indicated that in condensed phase systems, the hydration of H_3O^+ in the resultant H_3O^+–OH prompted it to separate into individual moieties [26, 27]. A series of studies on the ionization dynamics of water clusters have also been reported by our group [28–34]. The time-scale of ionization processes, e.g., the lifetime of reaction intermediates and proton transfer rate in ionized clusters, has been evaluated in previous studies. Tachikawa also studied the ionization dynamics of water on ice surfaces [35] and the effects of zero-point vibrational energy on the ionization dynamics of $(H_2O)_2$ [36].

In contrast to the monovalent ionization of water clusters, investigations on the multi-valence ionization of water clusters are limited. Jahnke et al. reported a pioneering study on the subject [37]. They found that intermolecular coulombic decay (ICD) of inner-valence-ionized $(H_2O)_2$ occurs through the ionization of a H_2O molecule followed by low-energy electron emission from another H_2O molecule. The ICD is faster than proton transfer between two H_2O molecules, and the ICD leads to the generation of two H_2O^+. Thürmer et al. studied the reaction dynamics of liquid water after core ionization by X-ray irradiation [38]. They showed that proton transfer between two H_2O molecules generates a Zundel-type intermediate $(H_2O–H–OH)^+$, and then further ionizes to form H_2O^+–H_2O^+ and H_3O^+–OH^+ dications. Slavíček et al. reported the simulation results of O 1s Auger electron spectra of $(H_2O)_5$ clusters [39]. Their calculations indicate that electron-transfer-mediated decay of water cluster was enhanced by ultrafast proton transfer. Additionally, the charge separation through proton transfer mediates Auger process leading to the formation of H_3O^+ and OH^+. Chalabala et al. studied the double ionization of $(H_2O)_2$ by means of real-time, time-dependent density functional theory-based Ehrenfest molecular dynamics with a generalized gradient approximation functional [40]. They calculated the population of reaction products as a function of time on the basis of the dynamics of doubly ionized $(H_2O)_2$ at the lowest electronic state and found that the dominant reaction channel was separated into two H_2O^+. Recently, Zhang et al. experimentally investigated the proton transfer dynamics of $(H_2O)_2$ following strong-field ionization using ultrashort laser pulses [41]. The first and second ionizations occurred within the same laser pulse under the conditions applied. They detected H_2O^+, H_3O^+ and OH^+ from $(H_2O)_2$ via double ionization. However, the mechanism of reaction following the multi-valence ionization of $(H_2O)_2$ remains unexplored. To understand the selectivity of the reaction channels leading to the above dissociation products, information on the time-scale of the reaction steps incorporated in the ionization is essential.

This study investigates the reaction dynamics of doubly charged states of water dimer, following the two-electron ionization of neutral water dimer $(H_2O)_2$, using a direct *ab initio* molecular dynamics (AIMD) method. We elucidate and compare the reaction process and time-scale of direct ionization and stepwise ionization, as described later. Furthermore, the dissociation of $(H_2O)_2^{2+}$ in the first excited state was examined to elucidate the effect of excitation energy on the subsequent dissociation process.

2. Computational methods

The fully optimized geometries of $(H_2O)_2$ were obtained using the second-order Møller–Plesset (MP2) method with the 6-311++G(d,p) basis set. The optimized geometries of the cation complex generated from the vertically ionized dimer $(H_2O)_2^+$ were also obtained at the same level of theory. The Gaussian 09 program package was used for geometry optimization [42]. The total energies of $(H_2O)_2$, vertically ionized states from the dimer ($(H_2O)_2^+$ and $(H_2O)_2^{2+}$), cation complex generated from $(H_2O)_2^+$ and its vertically ionized dication, first excited state of $(H_2O)_2^{2+}$, and final dissociation products (H_2O^+, H_3O^+, and OH^+) were also calculated at the same level of theory. The atomic charge was calculated using the natural population analysis method.

Direct AIMD calculations were carried out at the CAM-B3LYP/6-311++G(d,p) level. In this study, the following two reaction pathways were considered.

(I) Direct two-electron ionization: $(H_2O)_2$ is vertically ionized to form $(H_2O)_2^{2+}$, and $(H_2O)_2^{2+}$ then gives dissociation products.

(II) Stepwise two-electron ionization: $(H_2O)_2$ is once ionized to $(H_2O)_2^+$, and then $(H_2O)_2^+$ is converted to a more stable structure. Second, vertical ionization occurs.

The trajectories following ionization through (I) and (II) were propagated from the resultant dications. In addition, trajectory calculations starting from the first excited state of $(H_2O)_2^{2+}$ were carried out. The initial electron configuration for the trajectory calculation of excited $(H_2O)_2^{2+}$ was generated by the CASSCF(6,6) method.

To compare the relative translational energies of the reaction products, the direct AIMD calculations were carried out from several geometries of $(H_2O)_2$ and $(H_2O)_2^+$ generated at 10 K (the CAM-B3LYP/6-311++G(d,p)). The Nose-Hoover algorithm was used to maintain a constant temperature in each trajectory. The trajectories of the ionization processes were propagated at the CAM-B3LYP/6-311++G(d,p) level of theory. Further detailed settings of the calculations have been introduced in previous reports [43-45]. The program code for AIMD calculations was developed by our group.

3. Results and discussion

3.1. Structure and energy of water dimer $(H_2O)_2$ and its cation complex

Figure 1A illustrates the optimized structures of $(H_2O)_2$ calculated at the MP2/6-311++G(d,p) level of theory. Here, H_2O(d) and H_2O(a) denote the H-donor and H-acceptor water molecules, respectively. This dimer has a linear form with C_s symmetry. The hydrogen bond distance r_1 is 1.950 Å, and the O-O distance R_{OO} is 2.914 Å. The O-H distances of H_2O(d) (r_2 and r_3) were 0.966 Å and 0.959 Å, respectively. These structural parameters are almost similar to those obtained in previous work, and the positive charge of the low-lying $(H_2O)_2^+$ generated by the vertical ionization of $(H_2O)_2$ is localized at H_2O(d) [30]. The optimized structure of the $(H_3O\ldots OH)^+$ cation complex generated through hydrogen transfer from H_2O(d) to H_2O(a) is shown in figure 1B. The r_1, r_2, and r_3 distances are 1.050 Å, 1.447 Å, and 0.976 Å, respectively, and R_{OO} is 2.493 Å. The positive charge of this complex is localized at H_2O(a) [30]; this complex can be represented as an H_3O^+–OH radical-ion pair formed through proton transfer from H_2O(d) to H_2O(a).

The geometrical parameters obtained at the CAM-B3LYP/6-311++G(d,p) level are similar to that obtained at the MP2 level (Table S1 in Supplemental Material).

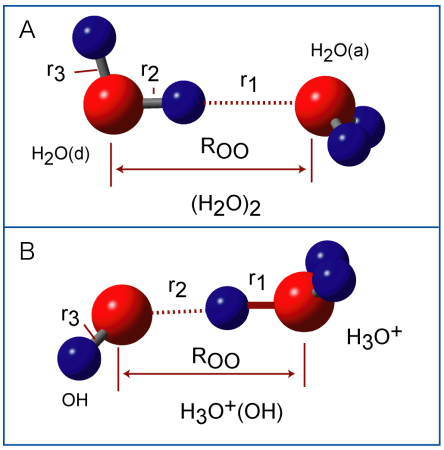

Figure 1. Optimized structures of neutral water dimer (A) and proton-transferred product (B) calculated at the MP2/6-311++G(d,p) level.

The total energies of all species involved in the reaction processes were also calculated at the MP2/6-311++G(d,p) level of theory. Figure 2 shows the energy diagram. In this diagram, the energy of neutral $(H_2O)_2$ before ionization was set to zero. In this study, direct AIMD calculations were started from states B (dimer dication formed by vertical ionization; direct ionization), C (excited state of the dimer dication; direct ionization on excites state), and E (dimer dication formed by the vertical ionization of the proton-transferred radical-ion pair; stepwise ionization).

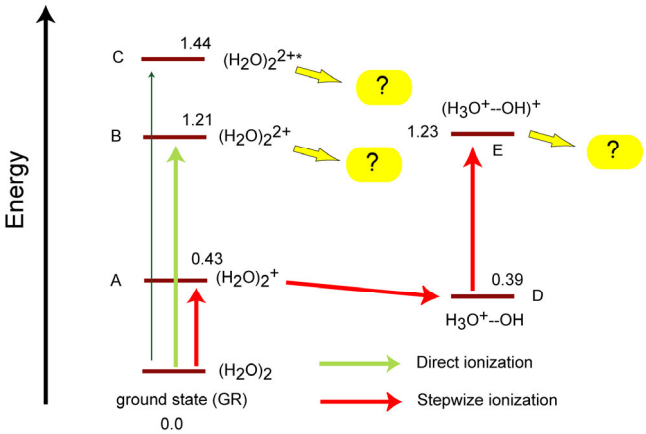

Figure 2. Energy diagram of the water dimer system calculated at the MP2/6-311++G(d,p) level. The values indicate the relative energies (in Hartree). The energy states A, B, and C mean the vertical ionized states from neutral dimer: one-electron ionized state of dimer (A), two-electron ionized state (B), and first excited state of two-electron ionized state (C). The states C and D mean the proton-transferred state from dimer: proton-transferred state from state A (D) and vertical excited state from state D (E).

3.2. Reaction dynamics of $(H_2O)_2^{2+}$ after direct two-electron ionization of $(H_2O)_2$ (direct ionization)

Figure 3 shows the snapshots and time evolution of the potential energy of $(H_2O)_2^{2+}$ following the vertical direct two-electron ionization of $(H_2O)_2$. The optimized structure obtained by MP2/6-311++G(d,p) was chosen as the initial geometry at time zero. The positive charges of H_2O(d) and H_2O(a) contained in $(H_2O)_2^{2+}$ at time zero were +1.08 and +0.92, respectively. This indicates that the positive charges are distributed almost equally on the two H_2O^+ ions. After ionization, these H_2O^+ ions separated from each other while rotating owing to the repulsion between the positive charges, the so-called Coulomb explosion. The potential energy monotonically decreased as the distance between the two H_2O^+ increased. The jagged shape of the potential energy curve is caused by the vibrational motion of the O–H stretching modes. The energy minimum found at 31.0 fs corresponds to the stabilization of the H_2O^+…H_2O^+ system caused by the structural change to give a face-to-face complex shown in figure 3A. Similar energy minima were found also at 145.6 fs and 260.0 fs, indicating that rotation happens periodically after 115 fs. After separation, the complex was dissociated. The relative translational energy of $H_2O^+ + H_2O^+$ system was calculated to be 40.6 kcal mol^{-1} at the CAM-B3LYP/6-311++G(d,p) level of theory. Figure S1 shows the potential energy curve in eV.

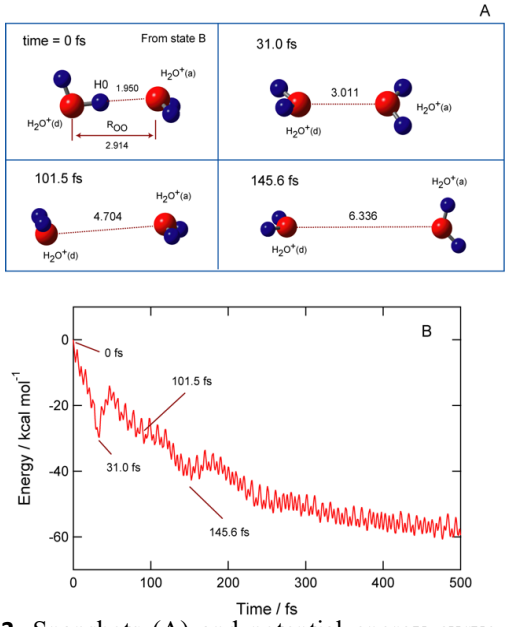

Figure 3. Snapshots (A) and potential energy curve (B) of $(H_2O)_2^{2+}$ following the vertical two-electron ionization from neutral water dimer. Direct AIMD calculations were carried out at the CAM-B3LYP/6-311++G(d,p) level. The MP2/6-311++G(d,p) optimized structure of the neutral water dimer was chosen as the initial structure at time zero. The values shown in (A) indicate the atomic distances in Å.

3.3. Reaction dynamics of $(H_2O)_2^{2+}$ after stepwise two-electron ionization of H_3O^+(OH) (stepwise ionization)

One-electron ionization of water dimer leads to the proton transferred radical-ion complex, H_3O^+(OH), as shown in Figure S2. The reaction is expressed as $(H_2O)_2^+ \rightarrow H_3O^+$(OH). The section investigates the reaction of $(H_2O)_2^{2+}$, following second ionization of H_3O^+(OH).

Figure 4 shows the snapshots and time evolution of the potential energy of $(H_2O)_2^{2+}$ following stepwise two-electron ionization of $(H_2O)_2$. The optimized structure obtained by MP2/6-311++G(d,p) was chosen as the initial geometry of H_3O^+(OH) at time zero. In this reaction channel, as described above, the H_3O^+–OH radical-ion pair is generated first (See, Figure S2). In this case, the AIMD calculations were started from the vertically ionized state of the radical-ion pair (state E). The positive charges of H_3O and OH contained in $(H_3O–OH)^{2+}$ at time zero were +0.96 and +1.04, respectively. This indicates that the positive charges were distributed almost equally on H_3O and OH. Consequently, this ionized state is represented as H_3O^+–OH^+. However, at this moment, the migrating proton is located around the midpoint between H_2O(d) and H_2O(a). After second ionization, r_1 shortened and R_{OO} elongated with time; H_3O^+ and OH^+ separated from each other. The potential energy monotonically decreased as the distance between H_3O^+ and OH^+ increased. The relative translational energy of $H_3O^+ + OH^+$ system was calculated to be 94.8 kcal mol^{-1} at the CAM-B3LYP/6-311++G(d,p) level of theory. Figure S3 depicts the potential energy curve in eV.

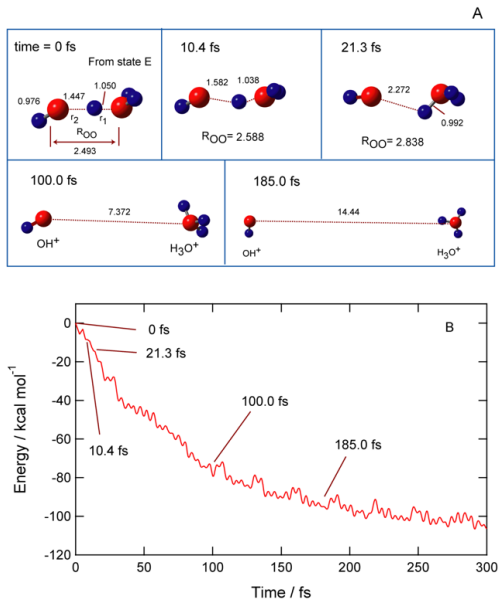

Figure 4. Snapshots (A) and potential energy curve (B) of $(H_2O)_2^{2+}$ following the vertical one-electron ionization from proton-transferred radical-ion pair (H_3O^+–OH). Direct AIMD calculations were carried out at the CAM-B3LYP/6-311++G(d,p) level. The MP2/6-311++G(d,p) optimized structure of H_3O^+–OH was chosen as initial structure at time zero. The values shown in (A) indicate the atomic distances in Å.

3.4. Reaction dynamics of $(H_2O)_2^{2+}$ after direct two-electron ionization to the first excited state $(H_2O)_2^{2+*}$(direct ionization on excited state potential energy surface (PES))

Figure 5 shows the snapshots and the time evolution of the potential energy of $(H_2O)_2^{2+}$ following direct two-electron ionization to the first excited state $(H_2O)_2^{2+*}$ (state C). The optimized structure obtained by MP2/6-311++G(d,p) was chosen as the initial geometry at time zero. The positive charges of H_2O(d) and H_2O(a) contained in $(H_2O)_2^{2+}$ at time zero were +0.89 and +1.11, respectively. The H-O-H angle of $H_2O(d)^+$ markedly increased after ionization, and H migrated from $H_2O(d)^+$ to $H_2O(a)^+$ within 50.5 fs. H_3O^+ and OH^+ were then formed. After the formation of H_3O^+ and OH^+, R_{OO} elongated over time, and the two ions separated from each other. The relative translational energy of the H_3O^+ + OH^+ system was calculated to be 86.3 kcal mol^{-1} at the CAM-B3LYP/6-311++G(d,p) level of theory. Potential energy curve in eV is given in Figure S4.

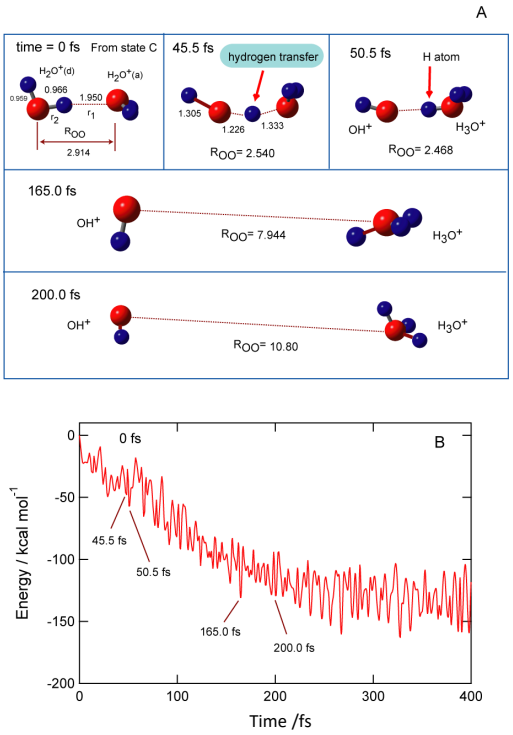

Figure 5. Snapshots (A) and potential energy curve (B) of $(H_2O)_2^{2+*}$ at first excited state following the vertical two-electron ionization from neutral water dimer. Direct AIMD calculations were carried out at the CAM-B3LYP/6-311++G(d,p) level. The MP2/6-311++G(d,p) optimized structure of neutral water dimer was chosen as initial structure at time zero. The values shown in (A) indicate the atomic distances in Å.

3.5. Summary of energy calculations

A complete energy diagram of the present study is shown in figure 6. As described above, all the reaction channels considered in this study gave the dissociation products. Direct two-electron ionization of $(H_2O)_2$ resulted in the formation of two H_2O^+ (state F), while stepwise ionization and direct ionization of $(H_2O)_2^{2+*}$ led to dissociation into H_3O^+ and OH^+ (state G). The reaction energies from B, C, and E states to the products were 175.7, 263.6, and 131.8 kcal mol^{-1}, respectively.

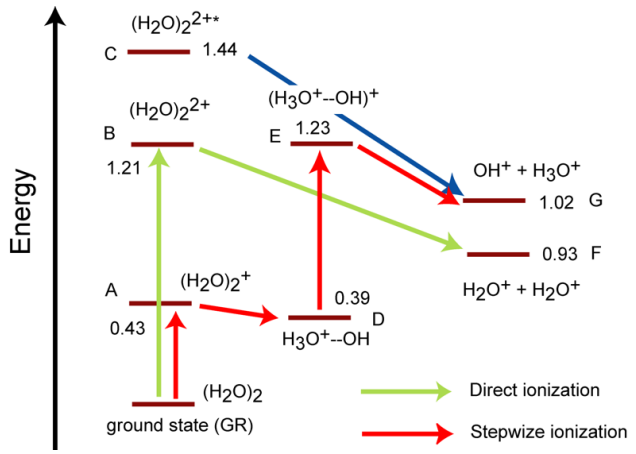

Figure 6. Summary of the present calculations. The values mean relative energies (in Hartree) calculated at the MP2/6-311++G(d,p) level.

3.6. Distribution of translational energies of dissociation products

The relative translational energies for direct, stepwise, and direct on excited PES were calculated to be 40.6, 94.8, and 86.3 kcal mol^{-1}, respectively. In the real system, the structure of the neutral dimer and ion-radical complex fluctuate around the equilibrium configurations due to thermal activation. In order to take into account thermal effects on these structures, direct AIMD calculations of of $(H_2O)_2$ and $(H_2O)_2^+$ were carried out under constant temperature conditions at the CAM-B3LYP/6-311++G(d,p) level. Temperature of 10 K was selected [44, 45]. From these simulations, several geometries were selected, and then direct AIMD calculations were run on vertical ionization points. Figure 7 shows the average translational energies of the dissociation products obtained through the reaction channels explained in previous section. The relative translational energies obtained from the trajectory calculations are summarized in table 1. The relative translational energy of $H_2O^+ + OH^+$ formed through stepwise ionization was approximately twice that of $H_2O^+ + H_2O^+$ formed through direct ionization. Direct ionization to the first excited state $(H_2O)_2^{2+*}$ led to the same dissociation products as those obtained through stepwise ionization, while the relative translational energies of the products derived from these reaction channels were different from each other. These results indicate that the reaction channels of two-electron ionization can be experimentally identified based on the difference in the translational energy distribution of the dissociation products.

In the present case, although the dissociation products of the stepwise ionization and those of the direct ionization to the first excited state are identical ($H_3O^+ + OH^+$), they are expected to be distinguished by experimental observations involving translational energy measurements. For example, time-of-flight mass spectroscopy (TOF-MS) can be applied for this purpose. TOF-MS has been used to detect the dissociation products of water. For example, Yuan, Yang and their coworkers applied TOF-MS to measure translational energies of products of vacuum ultraviolet photolysis of H_2O [46, 47]. Rocher-Casterline et al. used TOF-MS to elucidate the vibrational pre-dissociation dynamics of the HCl–H_2O dimer [48]. A similar technique is expected to be applied to investigate the mechanism of the ionization dynamics of $(H_2O)_2$.

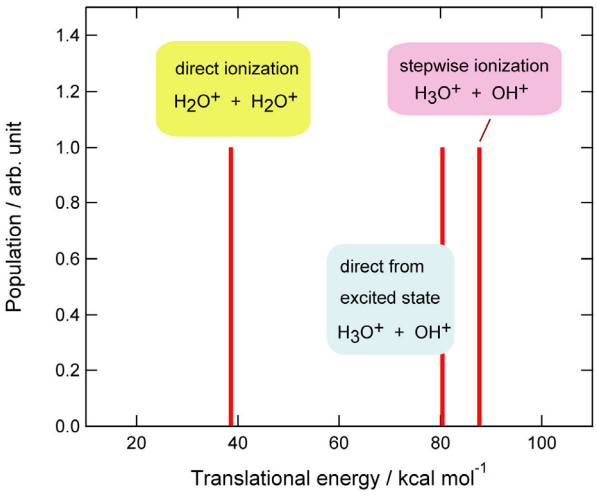

Figure 7. Relative translational energies (in kcal mol^{-1}) of products in each reaction channel. The calculations were carried out at the CAM-B3LYP/6-311++G(d,p) level.

Table 1. Average relative translational energies $<E_{tr}>$ of dissociation products calculated at the CAM-B3LYP/6-311++G(d,p) level. "No. of traj." means numbers of reactive trajectories led to products. The translational energies obtained from MP2 initial geometries are given in parenthesis.

Channel	Product	$<E_{tr}>$/kcal mol^{-1}	No. of traj.
Direct	$H_2O^+ + H_2O^+$	38.6 (40.6)	8
Stepwise	$H_3O^+ + OH^+$	87.7 (94.8)	9
Direct on excited PES	$H_3O^+ + OH^+$	80.4 (86.3)	3

4. Concluding remarks

This study revealed that the two-electron ionization states of $(H_2O)_2$ led to different dissociation products. In direct ionization, $(H_2O)_2^{2+}$ homogeneously dissociated to give two H_2O^+ ions; in the stepwise ionization, H_3O^+ and OH^+ were generated via proton-transferred H_3O^+–OH radical-ion pairs. In addition to the dissociation processes starting from low-lying dications, direct ionization to the first excited state of the dication $(H_2O)_2^{2+*}$ was investigated. Unlike direct ionization to the ground state $(H_2O)_2^{2+}$, the excited $(H_2O)_2^{2+*}$ dissociated to give H_3O^+ and OH^+. The dissociation processes following the two-electron ionization of $(H_2O)_2$ are summarized as follows:

- Direct ionization (ground state of vertically ionized dimer):

$$(H_2O)_2 + I_{P(D)} \rightarrow [(H_2O)_2^{2+}]_{ver} + 2e^- \quad (1)$$
$$[(H_2O)_22^+]_{ver} \rightarrow 2H_2O^+ \quad (2)$$

- Direct ionization (first excited state of vertically ionized dimer):

$$(H_2O)_2 + I_{P(D)} + E_{ver} \rightarrow [(H_2O)_2^{2+}]_{ver}^* + 2e^- \quad (3)$$
$$[(H_2O)_2^{2+}]_{ver}^* \rightarrow H_3O^+–OH^+ \rightarrow H_3O^+ + OH^+ \quad (4)$$

- Stepwise ionization (ground state of vertically ionized radical-ion pair)

$$(H_2O)_2 + I_{P(S1)} \rightarrow [(H_2O)_2^+]_{ver} + e^- \quad (5)$$
$$[(H_2O)_2^+]_{ver} \rightarrow H_3O^+–OH \quad (6)$$
$$H_3O^+–OH + I_{P(S2)} \rightarrow H_3O^+–OH^+ \rightarrow H_3O^+ + OH^+ \quad (7)$$

Here, $I_{P(D)}$, $I_{P(S1)}$, and $I_{P(S2)}$ denote the vertical ionization potentials for the two-electron ionization of $(H_2O)_2$, one-electron ionization of $(H_2O)_2$, and ionization of the radical-ion pair, respectively. E_{ver} denotes the first excitation energy of $(H_2O)_2^{2+}$. These results are consistent with those mentioned in the Introduction [40, 41]; it is theoretically predicted that $(H_2O)_2^{2+}$ at the lowest electronic state gives $H_2O^+ + H_2O^+$, while $(H_2O)_2^{2+}$ generated by strong-field laser pulse irradiation results in the formation of $H_3O^+ + OH^+$ via a proton-transferred intermediate. Chalabala et al. showed that the dominant process at lowest electronic state of $(H_2O)_2$ (i.e. dissociation into two H_2O^+) started at ~50 fs and ended within 100 fs [40]. The time-scale is consistent with the present calculation. We found that the direct ionization to the first excited state leads to H_3O^+ and OH^+. Therefore, the dissociation routes depend on the energy level of directly ionized $(H_2O)_2$, and is a novel finding of the study. The latter case, the formation of $H_3O^+ + OH^+$ via a proton-transferred intermediate, includes the influence of the laser pulse duration because the time-scale of the proton transfer and the laser pulse width are comparable. Zhang et al. suggested that possible ways to exclude the influence of pulse duration are the use of an extremely short laser pulse width and successive ionization using the pump-probe method [41]. The dynamics calculation of stepwise ionization in this work started from geometrically optimized H_3O^+–OH radical-ion pair as an initial structure. To observe the dissociation of H_3O^+–OH corresponding to present results, $(H_2O)_2$ and H_3O^+–OH should be successively ionized under irradiation with precise pulse interval. Ultrafast extreme ultraviolet (XUV) pulse is reported to be useful for the observation of dissociative ionization of diatomic molecules such as H_2, D_2, N_2, and I_2 [49, 50]. The XUV method will also apply to the dissociation of $(H_2O)_2$. By applying these techniques, the respective observation of the reaction processes giving $H_2O^+ + H_2O^+$ and $H_3O^+ + OH^+$ predicted in this work will be experimentally achieved.

Furthermore, a comparison of the translational energies of the dissociation products derived from the three reaction channels revealed that these reaction channels can be identified experimentally by measuring the translational energies. In particular, the final products of Eqs. (4) and (7) are identical, but their translational energies are different. For this purpose, cold-target recoil ion momentum spectroscopy (COLTRIMS) reaction microscope will be a powerful tool [51]. The COLTRIMS technique offers direct, precise determination of momentum vectors (i.e. energy and

scattering angle) of recoil ions and electrons generated through the ionization of atoms, molecules, and clusters. For example, the COLTRIMS reaction microscope revealed the momentum distributions of D^+, Ne^+, and electrons generated through the fragmentation of D_2 and Ne_2 [52]. Haxton et al. elucidated the dynamics of dissociative electron attachment of H_2O on the basis of *ab initio* calculation results and COLTRIMS results [53]. Identification of the ionization processes giving identical products based on translational energy distribution will be a subject of future experimental work.

In the present study, only dimers were considered throughout. However, the ionization processes of larger water clusters and small clusters surrounded by other water molecules are also important for understanding the reaction processes under real conditions. Although one-electron ionization processes of larger water clusters have already been extensively studied [29, 31-34], their multi-valence ionization has not been elucidated. Larger clusters may exist in vaporized water, liquid water, and ice; therefore, knowledge of the multiple electron ionization of these clusters is necessary to understand the experimental results for the detection of reaction products and measurement of translational energy. Despite the limited cluster size, the reaction dynamics of direct and stepwise two-electron ionization processes will provide important information regarding the fragmentation of water clusters caused by irradiation with ionizing radiation and/or short-wavelength ultraviolet light.

Data availability statement

All data that support the findings of this study are included in the article and the supplementary materials.

Acknowledgements

This study was financially supported by JSPS KAKENHI (Grant No. 18K05021 and Grant No. 21K04973).

ORCID IDs

Tomoya Takada https://orcid.org/0000-0002-5701-7140
Hiroto Tachikawa https://orcid.org/0000-0002-7883-2865

References

[1] Kouchi A, Yamamoto T, Kozasa T, Kuroda T and Greenberg J 1994 *Astron. Astrophys.* 290 1009
[2] Gudipati M S and Allamandola L J 2003 *Astrophys. J. Lett.* 596 L195 DOI: 10.1086/379595
[3] Molano G C and Kamp I 2012 *Astron. Astrophys.* 537 A138 DOI: 10.1051/0004-6361/201015868
[4] Yokochi R, Marboeuf U, Quirico E and Schmitt B 2012 *Icarus* 218 760 DOI: 10.1016/j.icarus.2012.02.003
[5] Ciesla F J 2014 *Astrophys. J. Lett.* 784 L1 DOI: 10.1088/2041-8205/784/L1
[6] Diken E G, Headrick J M, Roscioli J R, Bopp J C, Johnson M A and McCoy A B 2005 *J. Phys. Chem. A* 109 1487 DOI: 10.1021/jp044155v
[7] McCunn L R, Roscioli J R, Elliott B M, Johnson M A and McCoy A B 2008 *J. Phys. Chem. A* 112 6074 DOI: 10.1021/jp802172q
[8] Gardenier G H, Johnson M A and McCoy A B 2009 *J. Phys. Chem. A* 113 4772 DOI: 10.1021/jp811493s
[9] Miller Y, Thomas J L, Kemp D D, Finlayson-Pitts B J, Gordon M S, Tobias D J and Gerber R B 2009 *J. Phys. Chem. A* 113 12805 DOI: 10.1021/jp9070339
[10] Soloveichik P, O'Donnell B A, Lester M I, Francisco J S and McCoy A B 2010 *J. Phys. Chem. A* 114 1529 DOI: 10.1021/jp907885d
[11] Douberly G E, Walters R S, Cui J, Jordan K D and Duncan M A 2010 *J. Phys. Chem. A* 114 4570 DOI: 10.1021/jp100778s
[12] Guasco T L, Johnson M A and McCoy A B 2011 *J. Phys. Chem. A* 115 5847 DOI: 10.1021/jp109999b
[13] Vaida V 2011 *J. Chem. Phys.* 135 020901 DOI: 10.1063/1.3608919
[14] Bednarek J, Plonka A, Hallbrucker A and Mayer E 1998 *Radiat. Phys. Chem.* 53 635 DOI: 10.1016/S0969-806X(97)00272-7
[15] Shafer N and Bersohn R 1991 *J. Chem. Phys.* 94 4817 DOI: 10.1063/1.460566
[16] Liu K, Cruzan J D and Saykally R J 1996 *Science* 271 929 DOI: 10.1126/science.271.5251.929
[17] Shinohara H, Nishi N and Washida N 1986 *J. Chem. Phys.* 84 5561 DOI: 10.1063/1.449914
[18] Shiromaru H, Shinohara H, Washida N, Yoo H S and Kimura K 1987 *Chem. Phys. Lett.* 141 7 DOI: 10.1016/0009-2614(87)80082-9
[19] Mizuse K, Mikami N and Fujii A 2010 *Angew. Chem. Int. Ed. Engl.* 49 10119 DOI: 10.1002/anie.201003662
[20] Mizuse K and Fujii A 2011 *Phys. Chem. Chem. Phys.* 13 7129 DOI: 10.1039/c1cp20207c
[21] Mizuse K, Kuo J L and Fujii A 2011 *Chem. Sci.* 2 868 DOI: 10.1039/C0SC00604A
[22] Mizuse K and Fujii A 2013 *Chem. Phys.* 419 2 DOI: 10.1016/j.chemphys.2012.07.012
[23] Barnett R N and Landman U 1997 *J. Phys. Chem. A* 101 164 DOI: 10.1021/jp962761n
[24] Lee H M and Kim K S 2009 *J. Chem. Theor. Comput.* 5 976 DOI: 10.1021/ct800506q
[25] Svoboda O, Hollas D, Ončák M and Slavíček P 2013 *Phys. Chem. Chem. Phys.* 15 11531 DOI: 10.1039/c3cp51440d
[26] Herr J D, Talbot J and Steele R P 2015 *J. Phys. Chem. A* 119 752 DOI: 10.1021/jp509698y
[27] Herr J D and Steele R P 2016 *J. Phys. Chem. A* 120 7225 DOI: 10.1021/acs.jpca.6b07465
[28] Tachikawa H 2002 *J. Phys. Chem. A* 106 6915 DOI: 10.1021/jp020871q
[29] Tachikawa H 2004 *J. Phys. Chem. A* 108 7853 DOI: 10.1021/jp049269l
[30] Tachikawa H 2011 *Phys. Chem. Chem. Phys.* 13 11206 DOI: 10.1039/c0cp02861d
[31] Tachikawa H and Takada T 2013 *Chem. Phys.* 415 76 DOI: 10.1016/j.chemphys.2012.12.027

[32] Tachikawa H and Takada T 2015 *RSC Adv.* 5 6945 DOI: 10.1039/C4RA14763D
[33] Tachikawa H and Takada T 2016 *Chem. Phys.* 475 9 DOI: 10.1016/j.chemphys.2016.05.024
[34] Tachikawa H and Takada T 2016 *Comput. Theor. Chem.* 1089 13 DOI: 10.1016/j.comptc.2016.05.008
[35] Tachikawa H 2016 *Surf. Sci.* 647 1 DOI: 10.1016/j.susc.2015.11.011
[36] Tachikawa H 2017 *J. Comput. Chem.* 38 1503 DOI: 10.1002/jcc.24783
[37] Jahnke T, Sann H, Havermeier T, Kreidi K, Stuck C, Meckel M, Schöffler M, Neumann N, Wallauer R, Voss S, Czasch A, Jagutzki O, Malakzadeh A, Afaneh F, Weber Th, Schmidt-Böcking H and Dörner R 2010 *Nat. Phys.* 6 139 DOI: 10.1038/NPHYS1498
[38] Thürmer S, Ončák M, Ottosson N, Seidel R, Hergenhahn U, Bradforth S E, Slavíček P and Winter B 2013 *Nat. Chem.* 5 590 DOI: 10.1038/nchem.1680
[39] Slavíček P, Winter B, Cederbaum L S and Kryzhevoi N V 2014 *J. Am. Chem. Soc.* 136 18170 DOI: 10.1021/ja5117588
[40] Chalabala J, Uhlig F and Slavíček P 2018 *J. Phys. Chem. A* 122 3227 DOI: 10.1021/acs.jpca.8b01259
[41] Zhang C, Lu J, Feng T and Rottke H 2019 *Phys. Rev. A* 99 053408 DOI: 10.1103/PhysRevA.99.053408
[42] Frisch M J, Trucks G W, Schlegel H B, Scuseria G E, Robb M A, Cheeseman J R, Scalmani G, Barone V, Mennucci B, Petersson G A, Nakatsuji H, Caricato M, Li X, Hratchian H P, Izmaylov A F, Bloino J, Zheng G, Sonnenberg J L, Hada M, Ehara M, Toyota K, Fukuda R, Hasegawa J, Ishida M, Nakajima T, Honda Y, Kitao O, Nakai H, Vreven T, Montgomery Jr. J A, Peralta J E, Ogiaro F, Bearpark M, Heyd J J, Brothers E, Kudin K N, Staroverov V N, Kobayashi R, Normand J, Raghavachari K, Rendell A, Burant J C, Iyengar S S, Tomasi J, Cossi M, Rega N, Millam J M, Klene M, Knox J E, Cross J B, Bakken V, Adamo C, Jaramillo J, Gomperts T, Stratmann R E, Yazyev O, Austin A J, Cammi R, Pomelli C, Ochterski J W, Martin R L, Morokuma K, Zakrzewski V G, Voth G A, Salvador P, Dannenberg J J, Sapprich S, Daniels A D, Farkas O, Foresman J B, Ortiz J V, Cioslowski J and Fox D J 2009 *Gaussian09* Rev. D.01, Gaussian Inc., Pittsburgh, PA
[43] Tachikawa H 2020 *J. Phys. Chem. A* 124 3048 DOI: 10.1021/acs.jpca.0c01729
[44] Tachikawa H and Iyama T 2020 *J. Phys. Chem. A* 124 7893 DOI: 10.1021/acs.jpca.0c05688
[45] Tachikawa H and Kawabata H 2020 *J. Phys. Chem. A* 124 8421 DOI: 10.1021/acs.jpca.0c07109
[46] Cheng Y, Yuan K, Cheng L, Guo Q, Dai D and Yang X 2011 *J. Chem. Phys.* 134 064301 DOI: 10.1063/1.3554213
[47] Wang H, Yu Y, Chang Y, Su S, Yu S, Li Q, Tao K, Ding H, Yang J, Wang G, Che L, He Z, Chen Z, Wang X, Zhang W, Dai D, Wu G, Yuan K and Yang X 2018 *J. Chem. Phys.* 148 124301 DOI: 10.1063/1.5022108
[48] Rocher-Casterline B E, Mollner A K, Ch'ng L C and Reisler H 2011 *J. Phys. Chem. A* 115 6903 DOI: 10.1021/jp112024s
[49] Billaud P, Géléoc M, Picard Y J, Veyrinas K, Hergott J F, Marggi Poullain S, Breger P, Ruchon T, Roulliay M, Delmotte F, Lepetit F, Huetz A, Carré B and Dowek D 2012 *J. Phys B: At. Mol. Opt. Phys.* 45 194013 DOI: 10.1088/0953-4075/45/19/194013
[50] Kornilov O, Eckstein M, Rosenblatt M, Schulz C P, Motomura K, Rouzée A, Klei J, Foucar L, Siano M, Lübcke A, Schapper F, Johnsson P, Holland D M P, Schlathölter T, Marchenko T, Düsterer S, Ueda K, Vrakking M J J and Frasinski L J 2013 *J. Phys B: At. Mol. Opt. Phys.* 46 164028 DOI: 10.1088/0953-4075/46/16/164028
[51] Ullrich J, Moshammer R, Dörner R, Jagutzki O, Mergel V, Schmidt-Böcking H and Spielberger 1997 *J. Phys B: At. Mol. Opt. Phys.* 30 2917 DOI: 10.1088/0953-4075/30/13/006
[52] Czasch A, Schmidt L Ph H, Jahnke T, Weber Th, Jagutzki O, Schössler S, Schöffler M S, Dörner R and Schmidt-Böcking H 2005 *Phys. Lett. A* 2005 347 95 DOI: 10.1016/j.physleta.2005.08.043
[53] Haxton D J, Adaniya H, Slaughter D S, Rudek B, T. Osipov, Weber T, Rescigno T N, McCurdy C W and Belkacem A 2011 *Phys. Rev. A* 84 030701(R) DOI: 10.1103/PhysRevA.84.030701